

10-2-1991

## A Theory and Monte Carlo Calculation on Low Energy Electron Scattering in Solids

Yen-cai Ho  
*Shanghai Institute of Ceramics*

Zheng-yu Tan  
*Shandong Polytechnic University*

Xin-lei Wang  
*Shanghai Institute of Ceramics*

Jia-guang Chen  
*Shanghai Baoshan Steel Works*

Follow this and additional works at: <https://digitalcommons.usu.edu/microscopy>

 Part of the [Biology Commons](#)

---

### Recommended Citation

Ho, Yen-cai; Tan, Zheng-yu; Wang, Xin-lei; and Chen, Jia-guang (1991) "A Theory and Monte Carlo Calculation on Low Energy Electron Scattering in Solids," *Scanning Microscopy*: Vol. 5 : No. 4 , Article 5. Available at: <https://digitalcommons.usu.edu/microscopy/vol5/iss4/5>

This Article is brought to you for free and open access by the Western Dairy Center at DigitalCommons@USU. It has been accepted for inclusion in Scanning Microscopy by an authorized administrator of DigitalCommons@USU. For more information, please contact [digitalcommons@usu.edu](mailto:digitalcommons@usu.edu).



## A THEORY AND MONTE CARLO CALCULATION ON LOW ENERGY ELECTRON SCATTERING IN SOLIDS

Yen-cai Ho<sup>1\*</sup>, Zheng-yu Tan<sup>2</sup>, Xin-lei Wang<sup>1</sup>, and Jia-guang Chen<sup>3</sup>

<sup>1</sup> Shanghai Institute of Ceramics, Academia Sinica

<sup>2</sup> Shandong Polytechnic University

<sup>3</sup> Research Department, Shanghai Baoshan Steel Works

(Received for publication March 21, 1990, and in revised form October 2, 1991)

### Abstract

Low energy electron scattering (LEES) courses in solids are described by using a strict theory and direct simulation method proposed in this paper: we have improved Pendry's method based on the partial wave expansion, which can be applied to calculate the elastic scattering between an electron and atoms. The contributions of shell electrons, conductive electrons and plasma excitations are considered in the calculation of the inelastic scattering; electron scattering and cascade process of secondary electrons are simulated by Monte Carlo method. The secondary electron yields, the energy spectra curve and the backscattering electron coefficients for Cu were evaluated at the various energies, the theoretical results are in agreement with the Koshikawa's experiments.

### Introduction

Recently, much interest has arisen in the theoretical research, the calculation method and the practical applications of low energy electron scattering, which has become an active research field. The interaction between electrons and solids is a physical foundation of modern surface analysis technology, such as scanning electron microscopy (SEM), electron probe microanalysis (EPMA), and scanning Auger microscopy (SAM). When the primary energy of incident electron is tens of keV, the elastic scattering in solids can be described by Rutherford differential cross-section, and the Bethe equation based on the continuous energy loss is suitable for calculating the inelastic scattering. The Monte Carlo simulation based on the two principles has been successfully used to solve a series of difficult problems in the electron beam microanalysis and the electron beam lithography (4,5,6,7,10, 11) for many years. However, when the primary energy becomes several keV or lower, the Rutherford cross-section and the Bethe equation derived from the Born approximation are not applicable (9). The lower the energy (or the higher the atom number), the worse is their accuracy. In addition, the experimental techniques related to LEES, such as the low energy scanning electron microscopy and low energy electron beam lithography have developed quickly and bring about the advancements of surface analysis of solids and new technology on large-scale integration manufacture. Therefore, it is necessary for us to establish a strict physical model and a practical calculation method to deal with low energy electron scattering processes.

Kotera et al. calculated the electron scattering for Au below 10 keV using Mott elastic cross-section and the Kanaya energy loss equation (9), their results are more accordant with the experiments than those obtained by using the Rutherford-Bethe theories.

Shimizu and Ichimura have proposed a calculation method (14) to simulate the scattering processes of keV electrons penetrating into aluminum. In their model elastic scattering cross-section is derived by the partial wave expansion method considering the relativistic effect; inelastic scattering is divided into three different parts.

In this paper we have presented a Monte Carlo simulation to describe the scattering processes of low energy electrons in copper: 1) Pendry's calculation

**KEY WORDS:** Low energy electron scattering, Monte Carlo simulation, Backscattering coefficient, Secondary electron yield.

\*Address for correspondence:

Yen-cai Ho

865 Chang-ning Road,  
Shanghai 200050, China

Phone No. 21-2512990

method on elastic scattering has been improved, and 2) inelastic scattering is calculated by using the method in reference (14).

Elastic Scattering

Pendry's procedure (12) to calculate low energy electron elastic scattering based on the partial wave method of quantum mechanics is stricter, but there are several defects. We have made some improvements to Pendry's work and obtained a better calculation method, which will be published in another paper. Here is a summary of the calculations.

The differential scattering cross-section is acquired by solving the non-relativistic Schrodinger equation:

$$\frac{d(\sigma)}{d\Omega} = \frac{1}{k^2} \left| \sum_{l=0}^{\infty} (2l+1) \sin \delta_l \cdot \exp(i\delta_l) P_l(\cos\theta) \right|^2, \quad (1)$$

where  $k^2 = 2E$ ,  $E$  is incident electron energy,  $P_l(\cos\theta)$  is Legendre function,  $\delta_l$  represents the phase shift with angular momentum  $l$ , it is given by reference (1)

$$\delta_l = \arctan \left( \frac{j'_l - L_l j_l}{n'_l - L_l n_l} \right)_{r=R}, \quad (2)$$

where  $j_l(kr)$  and  $n_l(kr)$  are spherical function and spherical Neumann function, respectively;  $j'_l$  (or  $n'_l$ ) is derivative to  $r$ , and  $R$  is Muffin-tin radius. In addition

$$L_l = \left( \frac{d\Phi_l}{dr} / \Phi_l \right)_{r=R}, \quad (3)$$

in which,  $\Phi_l$  is the radial wave function of an incident electron.

The total elastic scattering cross-section is characterized by a set of phase shifts:

$$\sigma_{et} = \frac{4\pi}{k^2} \sum_{l=0}^{\infty} (2l+1) \sin^2 \delta_l. \quad (4)$$

We can see from equations (1) to (4), the calculations of the scattering cross-section  $\sigma_{et}$  is, in the final analysis, to evaluate the radial wave functions of an incident electron.

The non-overlapping sphere, taken as ion core potential by Pendry, is called 'Muffin-tin approximation'. Then, function  $\Phi_l$  satisfies

$$-\frac{1}{2r^2} \cdot \frac{d}{dr} \left( r^2 \frac{d\Phi_l}{dr} \right) + \frac{l(l+1)}{2r^2} \Phi_l + V_H(r) \Phi_l + \int V_{ex}^{(l)}(r, r') \Phi_l(r') r'^2 dr' = E \Phi_l, \quad (5)$$

where  $V_H(r)$  is Hartree potential:

$$V_H = V_S(r) - \frac{Z}{r} + \sum_{j_s} \frac{|\Psi_j(\vec{r}, S)|^2}{|\vec{r} - \vec{r}'|} d^3\vec{r}', \quad (6)$$

in which,  $V_S = -3r \left( \frac{3\rho(r)}{8\pi} \right)^{1/3}$ ,  $\rho(r)$  is electron density,

$\sum_{j_s} = \sum_j \cdot \sum_{S_j}$ ,  $\sum_{S_j}$  represents the summation of all shell

electrons, and  $d^3r$  is the integration in space.

Eq. (6) can not be calculated practically, using the quantum theory of atom structure we have derived the expression, which is convenient for digital computation:

$$V_H(r) = \frac{1}{r} [rV_S(r) - Z + 2 \left( \int_0^r \sum_{l'} (2l'+1) |\psi_{l'}(r')|^2 r'^2 dr' + r \int_r^\infty \sum_{l'} (2l'+1) |\psi_{l'}(r')|^2 r' dr' \right)], \quad (7)$$

where  $\psi_l$  is the electron radial wave function of an atom with trajectory quantum number  $l$ .

$V_{ex}(r, r')$  is called Hartree-Fock exchange potential. The calculated values may be too small for computer to express near the beginning point  $r_0$  in higher energy region. Let  $l'' = |l - l'|$ ,  $r_m = m_1 r^{l''}$ ,  $r'_m = m_1 r'^{l''}$ , then

$$\int V_{ex}^{(l)}(r, r') \Phi_l(r') r'^2 dr' = \sum_{l'}^{l+l''} c(l, l', l'') \left\{ \frac{\psi_{l'}(r)}{r \cdot r_m} \int_0^r \psi_{l'}^*(r') \Phi_l(r') r'^2 r'_m dr' + r_m \psi_{l'}(r) \int_0^\infty \psi_{l'}^*(r') \Phi_l(r') \frac{r'^l}{r'_m} dr' \right\}, \quad (8)$$

and

$$c(l, l', l'') = \frac{2l'+1}{2} \int_{-1}^1 P_l(u) P_{l'}(u) P_{l''}(u) du. \quad (9)$$

It will occur overflow in process of calculation when the electron energy  $E$  is larger than 1 keV, and  $l, l''$  are large enough. Thus, we introduce an exchange so that the calculation of function  $C(l, l', l'')$  can be carried out smoothly.

Let  $f_1 = r\Phi_l$ ,  $f_2 = f_1' - \frac{l+1}{r} f_1$ , then equation (5) is

written as follows

$$\begin{aligned} f_1' &= f_2 + \frac{l+1}{r} f_1 \\ f_2' &= 2(V_H - E) f_1 - \frac{l+1}{r} f_2 + 2V_g(r), \end{aligned} \quad (10)$$

in which

$$V_g(r) = r \int V_{ex}^{(l)}(r, r') \Phi_l(r') r'^2 dr'.$$

The primary solution of functions  $f_1$  and  $f_2$  is

$$\begin{aligned} f_1 &= C_0 r^{l+1} \left[ 1 - \left( \frac{Z}{l+1} \right) r + \alpha r^2 - \beta r^3 + \dots \right] \\ f_2 &= C_0 r^{l+1} \left[ 1 - \frac{Z}{l+1} + 2\alpha r - 3\beta r^2 + \dots \right], \end{aligned} \quad (11)$$

in which

$$\begin{aligned} \alpha &= \frac{Z^2 - (l+1)(E + V_0)}{(l+1)(2l+3)} \\ \beta &= \frac{Z(Z^2 - (3l+4)(E + V_0))}{3(l+1)(l+2)(2l+3)}. \end{aligned}$$

In Eq. (11)  $C_0$  is a constant, its value will affect the normalization factor of wave function  $\Phi_l$ . We can prove

that the value of  $C_0$  does not influence the calculated results of phase shifts, therefore, the overflow may be avoided by suitably adjusting  $C_0$ .

So far, a stricter method for calculating electron elastic scattering in a wide range of energy has been completed.

Using the partial wave method, we calculated the scattering cross-sections for Be, C, Al, Si and Cu at the different energies, and the ratio  $R_{p,r}$ ,  $(\frac{d\sigma}{d\Omega})_{p.w.m} / (\frac{d\sigma}{d\Omega})_R$ , between partial wave cross-section and Rutherford cross-section (Fig.1). The results show that the difference between both these cross-sections will increase with the decrease of the energy  $E$  or the increase of the atomic number. It is evident that Rutherford theory can not be applied to calculate low energy electron elastic scattering.

In addition, the contribution of Hartree-Fock exchange potential is studied in the paper. The elastic scattering cross-sections for Al and Cu with the energies from 0.5 to 5 keV are calculated by using Hartree and Hartee-Fock approximation respectively. We can see from the results for Cu shown in Table 1 that the lower the energy  $E$ , the larger is the influence of Hartree-Fock potential; when the energy increases to 1 keV, the difference between calculated values using Hartree-Fock and Hartree potential is very small. Therefore, we think Hartree-Fock approximation should be applied below 1 keV, when  $E$  is higher than 1 keV use of Hartree potential may also provide enough precision. Thus, we can save CPU time in computing.

### Inelastic Scattering

We take the stricter theories to replace Bethe continuous energy loss approximation to deal with low energy electron inelastic scattering. The inelastic scatterings resulted from ion core and conductive electrons consists of two parts: single electron excitation and plasma excitation. Single electron excitation includes shell electron excitation and conductive electron excitation.

#### Shell Electron Excitation

The equation of calculating shell electron excitation cross-section was derived by Gryzinski (3). When the electron energy loss is  $\Delta E$ , the differential scattering cross-section is:

$$\frac{d\sigma_s(\Delta E)}{d\Delta E} = \frac{K_j \pi e^4}{(\Delta E)^3} \left( \frac{E_j}{E + E_j} \right)^{3/2} \cdot \left( 1 - \frac{\Delta E}{E} \right)^{E_j / (E_j + \Delta E)} \cdot \left[ \frac{\Delta E}{E_j} \left( 1 - \frac{E_j}{E} \right) + \frac{4}{3} \ln \left( 2.7 + \left( \frac{E - \Delta E}{E_j} \right)^{1/2} \right) \right], \quad (12)$$

where  $E_j$  and  $K_j$  are the binding energy and the number of electrons of shell  $j$ , respectively.

The scattering cross-section,  $\sigma_{s_j}$ , of relative shell for Al and Cu at the different energies were calculated from Eq. (12) (Fig. 2).

The calculated results show that the ratios between L shell and M shell excitation cross-sections for Cu at 0.5—5 keV vary from 0, 0.0000182 to 0.00268, i.e. the maximum value is not more than 0.3%; and that is less than 0.4% for Si. It is proved that shell electron excitation principally occurs in the outer

shell.

#### Conductive electron Excitation

Streitwolf formula (15) for calculating conductive electron excitation is:

$$\frac{d\sigma_c(\Delta E)}{d\Delta E} = \frac{N \pi e^4}{E} \cdot \frac{1}{(\Delta E - E_F)^2}$$

$$\frac{d\sigma_c(\Delta E)}{d\Delta E} = 0.34 \frac{N \pi e^4}{E} \cdot \frac{1}{E_F^2}, \quad (13)$$

where  $N$  is Avogadro number, and  $E_F$  is the Fermi energy.

When energy loss  $\Delta E = E_F$ , the form of definite integral for evaluating the total cross-section is as follows:

$$\sigma_c = \int_{E_F}^{2.715 E_F} 0.34 \frac{N \pi e^4}{E} \cdot \frac{1}{E_F^2} d\Delta E$$

$$+ \int_{2.715 E_F}^E \frac{N \pi e^4}{E} \cdot \frac{1}{(\Delta E - E_F)^2} d\Delta E. \quad (14)$$

#### Plasma Excitation

Plasma excitation is a collective oscillation of conductive electrons related to ion cores, which resulted from incident electrons. The total cross-section is given by the equation (13) which is derived by 'quasi-particle approach':

$$\sigma_p = \frac{A}{N \rho} \cdot \frac{\hbar \omega_p}{2 a_0 E} \ln \left( \frac{\sqrt{E_F - \hbar \omega_p} - \sqrt{E_F}}{\sqrt{E_F} - \sqrt{E - \hbar \omega_p}} \right), \quad (15)$$

in which  $\hbar \omega_p$  is the plasma energy,  $A$  is atomic weight,  $\rho$  is the density, and  $a_0$  is the Bohr radius.

Then, kinds of inelastic scattering cross-sections are obtained, and the total inelastic scattering cross-section

$$\sigma_{it} = \sigma_s + \sigma_c + \sigma_p \quad (16)$$

The inelastic scattering cross-sections and the total values of Al and Cu in the range of low energy are shown in Fig. 3.

#### Monte Carlo Simulation

According to the principle mentioned above, a Monte Carlo method to calculate low energy electron scattering in solids has been established.

#### Scattering Free Length and Scattering Event

When electron energy is  $E$ , we calculate the elastic scattering and every inelastic scattering cross-sections of electrons, the total cross-section

$$\sigma_t = \sigma_{et} + \sigma_{it} = \sigma_{et} + \sigma_s + \sigma_c + \sigma_p. \quad (17)$$

The electron scattering free length

$$\lambda = - \frac{A}{N \rho \sigma_t} \ln R, \quad (18)$$

where  $R$  is a random number distributed homogeneously from 0 to 1.

The type of the next scattering event is determined by random sampling method when the free length  $\lambda$  is known.

To a given random number  $R$ , if

$$R < \sigma_{et} / \sigma_t ,$$

then, elastic scattering occurs;

$$\sigma_{et} / \sigma_t \leq R < (\sigma_{et} + \sigma_s) / \sigma_t ,$$

shell electron excitation;

$$(\sigma_{et} + \sigma_s) / \sigma_t \leq R < (\sigma_{et} + \sigma_s + \sigma_c) / \sigma_t ,$$

conductive electron excitation;

$$R \geq (\sigma_{et} + \sigma_s + \sigma_c) / \sigma_t ,$$

Plasma excitation.

#### Electron Angular Scattering and Energy Loss

The angle,  $\theta$ , of electron elastic scattering is obtained by random sampling:

$$R = \frac{\int_0^{\theta^*} \sin \theta d\sigma(\theta)}{\int_0^{\pi} \sin \theta d\sigma(\theta)} . \quad (19)$$

Combine equation (1) with the above formula, we have

$$R = \frac{\int_0^{\theta^*} \left| \sum_{l=0}^{\infty} (2l+1) \sin \delta_l \exp(i\delta_l) P_l(\cos \theta) \right|^2 \sin^2 \theta d\theta}{\int_0^{\pi} \left| \sum_{l=0}^{\infty} (2l+1) \sin \delta_l \exp(i\delta_l) P_l(\cos \theta) \right|^2 \sin^2 \theta d\theta} . \quad (20)$$

Since most inelastic scattering occurs in the excitation between incident electrons and conductive electrons or outer shell electrons, a free-electron model for binary collision is applicable to calculate inelastic scattering angle  $\theta_{in}$ :

$$\sin^2 \theta = \Delta E / E . \quad (21)$$

The energy loss  $\Delta E$  of inelastic scattering is obtained from random sampling similarly:

$$R = \frac{\int_{E_j}^{\Delta E} d\sigma(E)}{\int_{E_j}^{E_0} d\sigma(E)} . \quad (22)$$

where  $E_0$  is the primary energy of incident electrons.

#### Cascade Process

According to the principle mentioned above, the cascade process of low energy electron scattering in solids is simulated by Monte Carlo method. In the process, we trace every incident electron and the excited secondary electrons to calculate the next scattering and excitation until the electron leaves the surface of solids or stops in solids owing to its energy being dissipated. When  $E < E_F + W_F$  (work function), the electron is not tracked further. While the electron escapes from the surface, it must overcome the surface potential barrier. The electrons are roughly divided into the backscattering electrons (energy greater than 50 eV) and the secondary electrons (energy less than 50 eV)

The space transport process of electron scattering is calculated by the method in Ref.(2).

According to the principle of free electron approximation, the new coordinates of the excited conductive electrons, shell electrons and incident electrons after scattering can be determined by solving the momentum conservation equation of binary collision.

The electrons that escape from the surface should satisfy:

$$0 \leq \gamma \leq \arccos \left( \frac{E_F + W_F}{E} \right)^{1/2} , \quad (23)$$

where  $\gamma$  is the angle between scattering direction of electrons and the normal of surface. It is obvious that the larger the energy, the greater is the possibility to escape the surface.

#### Calculation Results and Discussion

Using the theory and calculation method in this paper, the backscattering coefficient  $\eta$ , the secondary electron yield  $\delta$  and its energy distribution are evaluated for Cu at the energy range of 100–3000 eV, and with varying the incident angle from  $0^\circ$  to  $60^\circ$ .

The calculated results are in agreement with the experimental values of Koshikawa and Shimizu (8). The calculated backscattering coefficient  $\eta$  for Cu is shown in Fig. 4.  $\eta$ - $E_0$  curve with normal incidence and the different incident angles are in accordance with K-S experiments (Fig. 4a, 4b) except that the calculated values are a little high.

We have calculated the secondary electron yield for Cu, when the energy  $E_0$  is 100, 200, 300, 400, 500, 1000, 2000 and 3000 eV, respectively. The results show that the value of  $\delta$  reduces as the energy decreases, and the maximum of  $\delta$  occurs at 500 eV (Fig. 5a). It is an important characteristic on the secondary electron emission, and has been proved by K-S experiments. The secondary electron energy spectra for Cu at 500 eV is shown in Fig. 5b. The calculated spectra curve is shifted to the side of low energy about 1 eV as compared with the experimental curve, however, the distribution of the two curves is accordant. when  $E_0$  is 1, 2, and 3 keV respectively, and the incident angle  $\theta_0$  varies from  $0^\circ$  to  $60^\circ$ , the calculated curves show the same distribution regularity. This is also an important characteristic on secondary electron emission.

It is possible to extend both our theory and calculation method to simulate low energy electron scattering in polybasic alloy, and to calculate the scattering processes in multi-layer medium. We are applying the method to the calculation of low energy electron beam lithography, in order to carry out some necessary theoretical analysis for the studies in this important technology field. It will be a very complex problem on low energy electron scattering in polybasic and multi-layer medium.

The Monte Carlo calculation was carried out on IBM 4381 computer, the simulated electron number is 5000.

Calculation of LEES in Solids

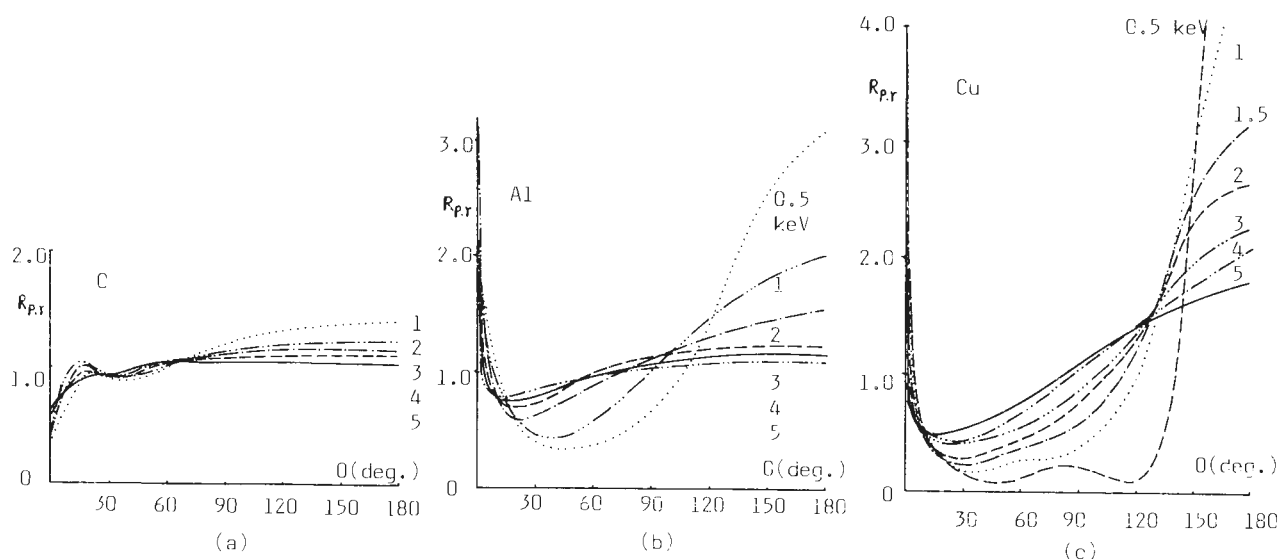


Fig. 1. The ratio  $R_{PR}$  between P.W.M cross-section and Rutherford cross-section at the different energies. (a), (b) and (c) are the calculated results for C, Al and Cu, respectively.

$E(\text{keV})$ $\sigma_T(\text{cm})$	0.5	1.0	2.0	3.0	4.0	5.0
$\sigma_{T.H}$	$0.1473 \times 10^{-15}$	$0.1081 \times 10^{-15}$	$0.8067 \times 10^{-16}$	$0.6440 \times 10^{-16}$	$0.5427 \times 10^{-16}$	$0.4715 \times 10^{-16}$
$\sigma_{T.HF}$	$0.1540 \times 10^{-15}$	$0.1100 \times 10^{-15}$	$0.8101 \times 10^{-16}$	$0.6457 \times 10^{-16}$	$0.5438 \times 10^{-16}$	$0.4725 \times 10^{-16}$
$\sigma_{T.H}/\sigma_{T.HF}$	0.9562	0.9843	0.9957	0.9973	0.9977	0.9979

Table 1. The scattering cross-sections for Cu calculated by Hartree ( $\sigma_{T.H}$ ) and Hartree-Fock ( $\sigma_{T.HF}$ ) approximation, respectively.

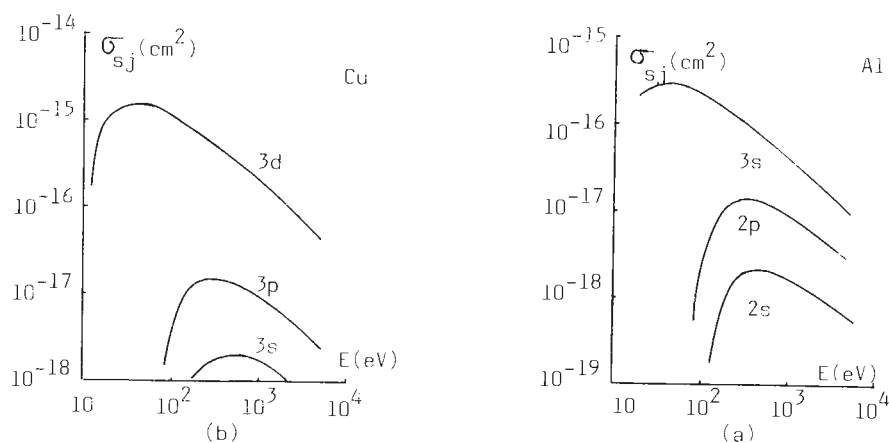


Fig. 2. Shell excitation cross-sections for Al and Cu in the range of low energy.

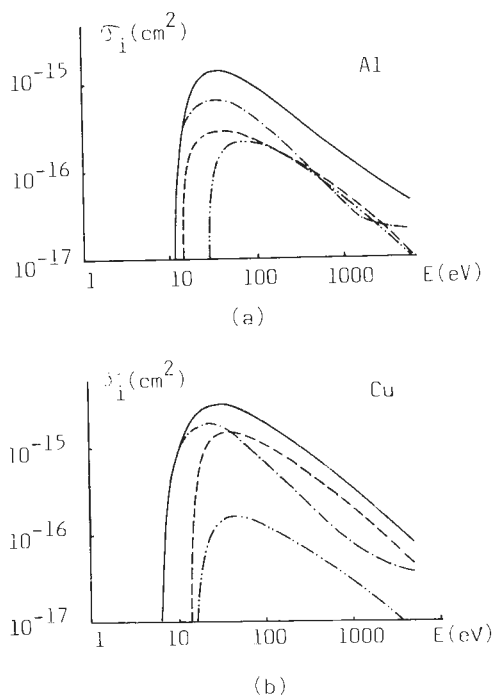


Fig. 3. Inelastic scattering cross-section and the total values of Al(a) and Cu(b),  
 —  $\sigma_{it}$ , - -  $\sigma_c$ , - · -  $\sigma_s$ , ···  $\sigma_p$

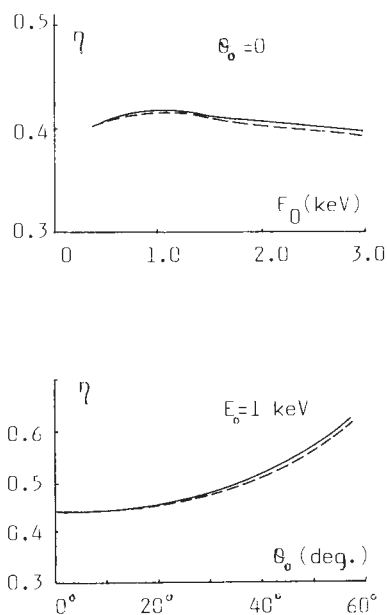


Fig. 4. Comparison of the calculated values and the experimental results of backscattering coefficient  $\eta$  for Cu.  
 — Calculated values,  
 ····· K-S experimental results.

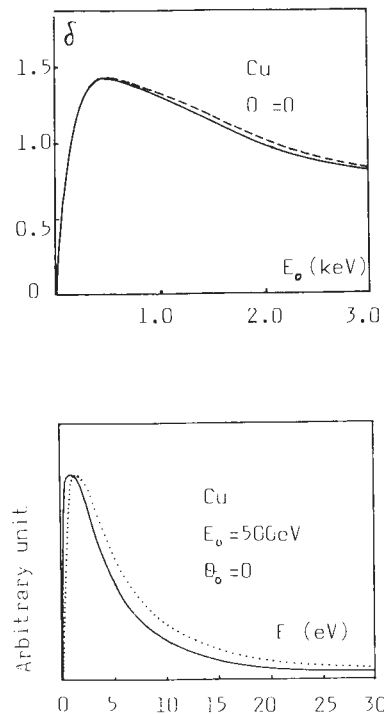


Fig. 5. The calculated secondary electron yield and energy spectra curve compared with the experimental results.  
 — Calculated values,  
 ····· experimental results.

References

1. Charles JJ(1975). Quantum Collision Theory, Amsterdam, North Holland Pub. Co., 81.
2. Curgenvan L, and Duncumb P(1971). Simulation of electron trajectories in a solid target by a simple Monte Carlo technique, Tube Investment Research Report 303.
3. Gryzinski M(1965). Two-Particle collision I, II, III, Phys. Rev., A, 138, 305-358.
4. Hawryluk RJ, Hawryluk AM, and Smith HI (1974) Energy dissipation in a thin polymer film by electron beam scattering, J. Appl. Phys., 45, 2551-2566.
5. Ho YC, Chen JG, and Wang XL (1987). A calculation method for quantitative X-ray microanalysis for microparticle specimens by Monte Carlo simulation, Scanning Microscopy, 1, 943-950.
6. Ho YC, Wang XL, and Chen JG (1988). A calculation method of XQMA for irregular-shaped super-microparticle specimens by Monte Carlo direct simulation, Scientia Sinica (Science in China), Series A, 31, 870-878.

7. Ho YC, Chen JG, and Wang XL (1989). An analytical method of determining thickness of multi-layer films with electron microprobe, *Scanning Microscopy*, **3**, 1009-1012.
8. Koshikawa T, and Shimizu R (1973). Secondary electron and backscattering measurements for polycrystalline copper with a spherical retarding-field analyser, *J. Phys. D: Appl. Phys.*, **6**, 1369-1380.
9. Kotera M, Murata, K, and Nagami K (1981). Monte Carlo simulation of 1-10-keV electron scattering in a gold target, *J. Appl. Phys.*, **52**, 997-1003.
10. Love G, Cox MGC, and Scott VD (1977). A simple Monte Carlo method for simulating electron-solid interactions and its application to electron probe microanalysis, *J. Phys. D: Appl. Phys.*, **10**, 7-23.
11. Murata K, Matsukawa T, and Shimizu R (1971). Monte Carlo calculation on electron scattering in a solid target, *J. Appl. Phys. Japan*, **10**, 678-686.
12. Pendry JB (1974). *Low energy electron diffraction*, Academic Press Inc. Ltd., London, 31-57.
13. Quinn JJ (1962). Range of excited electrons in metals, *Phys. Rev.*, **126**, 1453-1457.
14. Shimizu R, and Ichimura S (1982). Direct Monte Carlo simulation of kV electron scattering processes-N(E) spectra for aluminum, Proc. of the 1st Pfefferkorn Conf. on Electron Beam Interactions with Solids for Microscopy, Microanalysis and Microlithography, eds. D.F. Kyser, H. Niedrig, D.E. Newbury, and R. Shimizu, 165-172.
15. Streitwolf HW (1959). Zur Theorie der Sekundar Elektronen Emission von Metallen, Anregungsprozesse, *Ann. Phys. Leipzig*, **3**, 183-196.

D. E. Newbury: The agreement between the experimental results of Koshikawa and Shimizu and your Monte Carlo calculations shown in Figure 4 is quite impressive. Most Monte Carlo simulations have at least one parameter which must be adjusted to give close agreement with selected experimental data such as backscatter coefficients as a function of atomic number. After adjustment, further comparisons are made to other types of experimental data, such as transmission through thin foils, etc. Does your simulation require any such adjustment, or do the mathematical expressions for elastic and inelastic scattering directly produce such a good agreement?

Authors: This is a very interesting and essential question. There are always some deviations in Monte Carlo simulation of a physical process, which are resulted from the selection of a physical model and the random calculation. So Monte Carlo simulation usually have at least one parameter, which must be adjusted to obtain close agreement with experimental data. In our simulation of low energy electron scattering, the factor of inelastic scattering angle is set up to obtain good agreement with the experimental data of backscattering coefficient  $\eta$  and secondary electron yield  $\delta$ . From equation (21),  $\theta_{in} = \arcsin(\Delta E/E)^{1/2}$ . In simulation we let  $\theta_{in} = P_{\theta} \arcsin(\Delta E/E)^{1/2}$ .  $P_{\theta}$  is adjusted according to the experimental values of  $\eta$  and  $\delta$ .

Discussion with Reviewers

K. Murata: Please explain briefly on how you obtain the Muffin-tin radius.

Authors: We take the largest possible non-overlapping spheres drawn about each nucleus, the potential inside will be spherically symmetric, and the potential outside will be constant. A radius of the non-overlapping spheres is taken as the Muffin-tin radius.

K. Murata: Your calculations of the elastic scattering cross-section are based on the non-relativistic theory. Could you comment on how accurate your theory is, compared with the relativistic theory?

Authors: The calculated results of elastic scattering cross-section using the non-relativistic theory are less than those using the relativistic theory, and the difference between both these results will increase with the increase of the atomic number. Both calculated values are given in Tab. A.

Element		Relativistic	Non-relative	Deviation
Al	1 keV	$0.95 \times 10^{-16}$	$0.83 \times 10^{-16}$	12.6%
	3 keV	$4.24 \times 10^{-17}$	$3.98 \times 10^{-17}$	6.1%
Cu	1 keV	$1.48 \times 10^{-16}$	$1.09 \times 10^{-16}$	26.4%

Tab. A Comparison between our non-relativistic results and the relativistic values calculated by Shimizu et al. (*Surface Science*, 1981, **112**, 386-408).



